Structure, Mechanical, and Fracture Properties of Nanoreinforced and HNBR-Toughened Polyamide-6

Suchart Siengchin,[1] József Karger-Kocsis[2,3]

[1]*The Sirindhorn International Thai-German Graduate School of Engineering (TGGS), Production Engineering Department, King Mongkut's University of Technology North Bangkok, Bangsue, Bangkok 10800, Thailand*
[2]*Department of Polymer Technology, Faculty of Engineering and Built Environment, Tshwane University of Technology, Pretoria 0001, Republic of South Africa*
[3]*Department of Polymer Engineering, Faculty of Mechanical Engineering, Budapest University of Technology and Economics, H-1111 Budapest, Hungary*

Received 2 December 2010; accepted 19 March 2011
DOI 10.1002/app.34526
Published online 9 August 2011 in Wiley Online Library (wileyonlinelibrary.com).

ABSTRACT: Hydrogenated nitrile rubber (HNBR) and synthetic nanofillers, viz. water-swellable sodium fluorohectorite (FH) and water dispersible boehmite alumina (BA), were used to toughen and reinforce polyamide-6 (PA-6). FH and BA were introduced in HNBR latex that was dried prior to melt mixing with PA-6. Binary blend (PA-6/HNBR) and ternary nanocomposites (PA-6/HNBR/nanofiller) were produced and their structure–property relationships studied. HNBR was coarsely and microscale dispersed in PA-6. FH, slightly intercalated, was present in PA-6 and in the PA-6/HNBR interphase, whereas BA was mostly located in the HNBR droplets. HNBR improved the ductility of the PA-6/HNBR blend at cost of stiffness and strength. The fracture toughness and energy, determined on notched Charpy specimens at different temperatures ($T = -30°C$, room temperature, and $T = 80°C$) were improved by blending with HNBR at 9 wt %. Additional incorporation of the nanofillers in 2.5 wt % enhanced the stiffness and strength of the PA-6/HNBR blend but reduced its ductility. The fracture toughness of the ternary nanocomposites was between those of PA-6 and PA-6/HNBR, whereas their fracture energy fairly agreed with that of the parent PA-6.
 J Appl Polym Sci 123: 897–902, 2012

Key words: polyamide-6; hybrid nanocomposites; fracture toughness; toughening; structure–property relationships

INTRODUCTION

Incorporation of nanoparticles in thermoplastics may result in excellent mechanical, thermal, and other properties (e.g., enhanced heat distortion temperature, improved stiffness and strength, flame resistance and electric conductivity). A variety of nanofillers, such as clay, barium titanate, and multiwall carbon nanotube, has already been checked as possible reinforcements in polyamide-6 (PA-6; e.g.,[1–5]). The reinforcing action is given by the shape (aspect ratio) and high specific surface of the nanofillers when good adhesion between the filler surface and matrix exists.

Beside of traditional melt compounding, other techniques (e.g., solution blending, *in situ* polymerization) were also explored to improve the dispersion of the nanofillers. For rubbers and thermoplastics the water-mediated dispersion of suitable nanofillers has been recommended ([6]and references therein). This was fuelled by the fact that many rubbers are available in latex form and water can be a suitable carrier for given additives, to be incorporated in thermoplastics via melt blending operations. During the latter, the water is evaporated (supported by the local screw configuration and using auxiliary vacuum pump at the related outlet of the extruder) which is accompanied with a bubble-induced disintegration of the filler agglomerates. This is straightforward not only from the viewpoint of the dispersion of the nanofillers but also in respect to the reduction of health hazard.

It was demonstrated that the creep response of PA-6 nanocomposites strongly depends on the aspect ratio of the nanofillers used. Platy synthetic layered silicate [e.g., sodium fluorohectorite (FH)] of very high aspect ratio outperformed the flake-type synthetic boehmite alumina (BA) of low aspect ratio, when incorporated via water-assisted melt compounding in PA-6.[6] However, nanoreinforcement of

Correspondence to: S. Siengchin (suchart.s.pe@tggs-bangkok.org)

This work was performed in the framework of the project Development of quality-oriented and harmonized R + D + I strategy and functional model at BME, supported by the New Hungary Development Plan (Project ID: TÁMOP-4.2.1/B-09/1/KMR-2010-0002). Part of this work is also linked with a bilateral collaboration between the Republic of South Africa and Hungary.

thermoplastics is usually associated with toughness reduction.[7] On the other hand, the toughening of PAs is a well studied topic. Toughening of PAs via melt compounding with various rubbers (e.g., ethylene–propylene copolymer, ethylene–propylene–diene terpolymer, styrene–ethylene/butadiene–styrene—with and without various functional groups for improved compatibility with PA) belongs to the state-of-art.[8–10] Hydrogenated nitrile rubber (HNBR), being one of the most stable rubbers, has also been tried as toughener in PAs.[11] HNBR is a preferred component of temperature and oil-resistant thermoplastics elastomers of blend type, which often contain PAs as thermoplastics.[12,13] Rubber incorporation, however, reduces the stiffness and strength characteristics of the related compounds.

Our aim was to produce toughened PA-6 nanocomposites with balanced toughness and stiffness/strength properties by introducing both the nanofiller and toughening agent from aqueous dispersions. To support the dispersion of hydrophilic nanofillers, a variant of the water-mediated techniques has been followed. HNBR latex, being an aqueous dispersion of submicron sized rubber particles, was selected as a carrier for the water-swellable synthetic layered silicate (namely FH) and water-dispersible BA, respectively. The batch technique followed in this work can be considered as part of a feasibility study to develop a continuous melt compounding process with in-line modification possibilities (reinforcing and/or toughening of thermoplastics).

Accordingly, the goal of this study was to produce PA-6/HNBR(9 wt %)/nanofiller (2.5 wt %) ternary composites by melt mixing with a "masterbatch," received after drying the HNBR latex that contained the nanofillers and to determine the structure, mechanical, and fracture properties of the resulting compounds. To get a clear picture on the effect of the nanofillers, the structure, and properties of the PA-6/HNBR(9 wt %) were also studied. The latter binary composition was produced by melt blending of PA-6 with HNBR that was received after drying the corresponding latex.

EXPERIMENTAL

Materials and preparation of composites

Water dispersible BA (AlO(OH)) and water-swellable sodium FH ($(Mg_{5,2}Na_{0,8})(Si_8)O_{20}(OH)_{4-x}(F)_xNa_{0,8}$) were used as nanofillers. The nominal particle size of BA (Dispal® 11N7-80, Sasol GmbH, Hamburg, Germany) in water was 220 nm though that of the BA powder, as delivered, was $\sim$ 40 μm. The nominal aspect ratio of BA, being flake-type, is close to 1. FH (Somasif ME-100, Coop Chemicals, Tokyo, Japan) is characterized by an interlayer distance of 0.92 nm and a cation exchange capacity of 100 mequiv/100g. The nominal aspect ratio of FH, being plate-like, is close to 1000. HNBR latex with 40 wt % dry rubber content (Zetpol ZLX-A) was supplied by Zeon Corp. (Tokyo, Japan). This latex (acrylonitrile content of 38%) served as swelling and dispersing agent for the nanofillers. Note that HNBR was foreseen to act as impact modifier in the PA-6, as well. Granulated PA-6 (Ultramid® BS 700, BASF, Ludwigshafen, Germany) was selected as polymeric matrix for all composite systems. Its density and melting temperature were 1.15 g/cm^3 and 220°C, respectively.

PA-6/HNBR binary blend was produced by melt compounding using dry HNBR. The HNBR content in the corresponding blend was set for 9 wt %. PA-6-based ternary nanocomposites were prepared as follows. First, an aqueous slurry of FH or BA (10 wt %) was prepared at ambient temperature through mechanical stirring for 5 h or 30 min, respectively. Then, the rubber latex was introduced in this slurry and stirred for additional 30 min. The resulting slurry was poured in a framed glass plate and dried for 5 days at room temperature. The resulting dry nanofiller masterbatch was introduced in the PA-6 melt in a laboratory kneader (Type 50 of Brabender, Duisburg, Germany) at $T = 250$°C at a rotor speed of 60 revolutions per minute, rpm) after melt mastication of PA-6 granules for 2 min. The overall duration of the melt mixing was 6 min. The HNBR and nanofiller (FH or BA) content of the ternary composites were 9 and 2.5 wt %, respectively.

Characterization and testing

The dispersion of nanofillers and HNBR in the PA-6 nanocomposites was studied by inspecting the fracture surface of the specimens in a scanning electron microscope (SEM; JSM 5400, Jeol, Tokyo, Japan). The surface was gold coated prior to SEM inspection performed at low acceleration voltage. Transmission electron microscopy (TEM) measurements were carried out with a Zeiss LEO 912 Omega device (Oberkochen, Germany) applying an acceleration voltage of 120 kV. Thin sections ($\sim$ 50 nm) for TEM study were cut at room temperature with a Diatome diamond knife (Hatfield, PA) using an Ultracut E microtome (Reichert and Jung, Vienna, Austria).

X-ray diffraction (XRD) spectra were collected on a Siemens D5000 diffractometer (Karlsruhe, Germany) with Cu K_α (40 kV, 30 mA) radiation and a secondary-beam graphite monochromator. The spectra were recorded in the scatter range of $2\theta = 1.2$–$10°$ in steps of 0.05° with a counting time per steps of 10 s.

Tensile tests were performed on dumbbell-shaped specimens (DIN-ISO-527) in a Zwick 1474 (Ulm, Germany) universal testing machine. Tests were run at

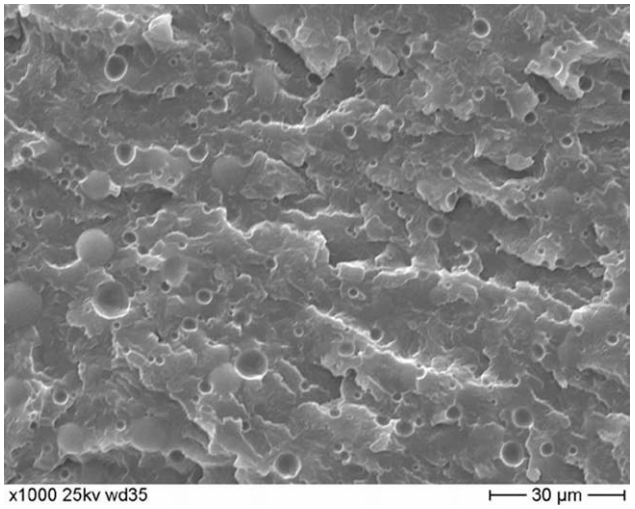

Figure 1 SEM picture from the fracture surfaces of PA-6/HNBR.

room temperature at $v = 2$ mm/min crosshead speed and the related stress–strain curves were registered.

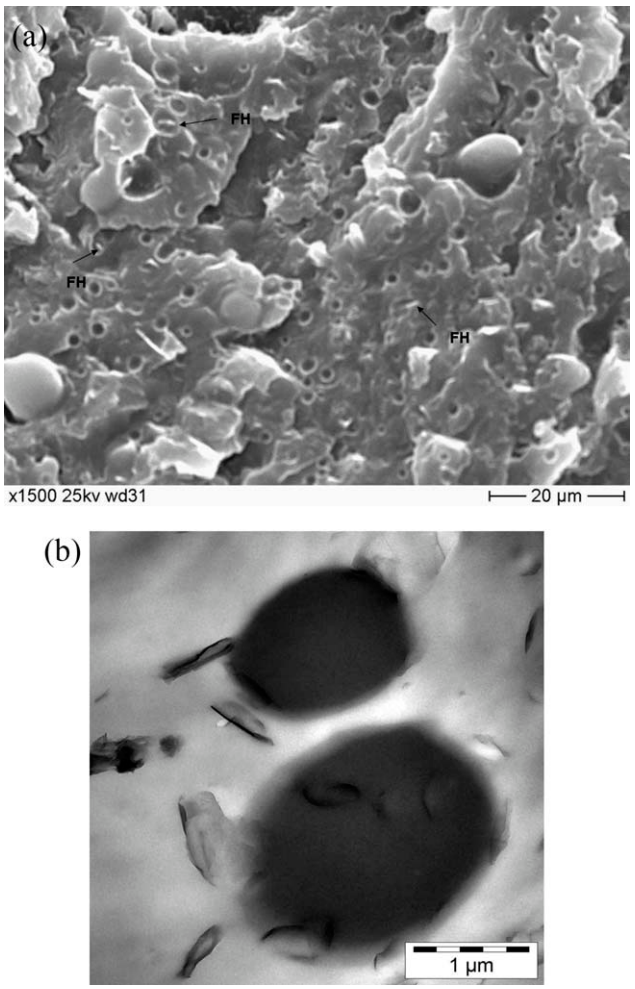

Figure 2 SEM (a) and TEM (b) pictures from the fracture surface and thin section, respectively, of PA-6/HNBR/FH.

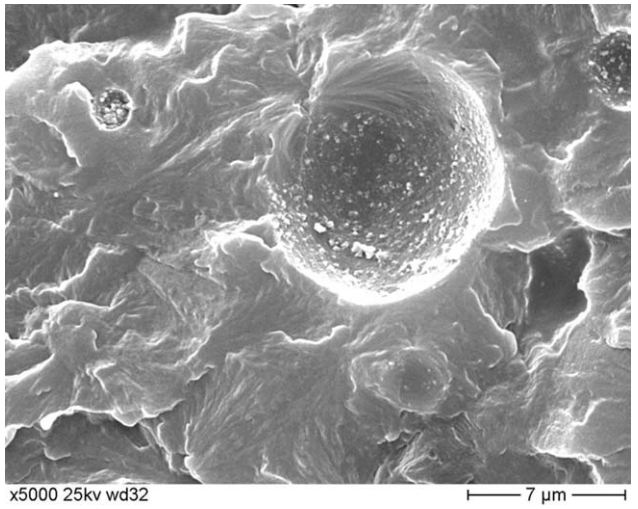

Figure 3 SEM picture from the fracture surfaces of PA-6/HNBR/BA.

Charpy tests were performed at $v = 1$ m/s at temperatures of -30°C, room temperature (RT), and 80°C, respectively, on notched specimens. The notch length to width ratio (a/w) of the Charpy specimens was constant, viz. 0.5. Notch was introduced by a V-type saw blade (Mutronic GmbH, Rieden, Germany). Instrumented impact test was performed on a pendulum (Ceast Spa, Pianezza, Italy) equipped with a data acquisition unit (DAS 800 of Ceast). The instrumented impact tests were done by cushioning the hammer edge with plasticine (impact energy: 0.48 J, hammer mass: 0.949 kg, and striker length: 0.23 m). The registered fractograms served to determine the dynamic fracture toughness (Kd) and energy (Gd) according to the ISO 17281:2002 standard (plastics—determination of fracture toughness at moderately high loading rates). The related test results represent average values received in five parallel tests.

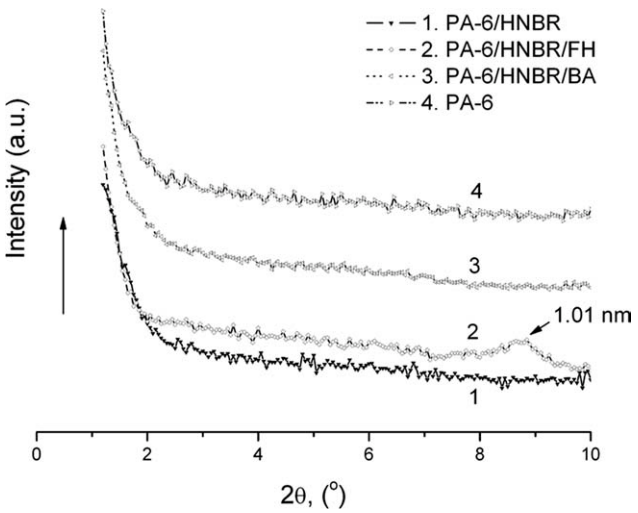

Figure 4 XRD spectra of the systems studied.

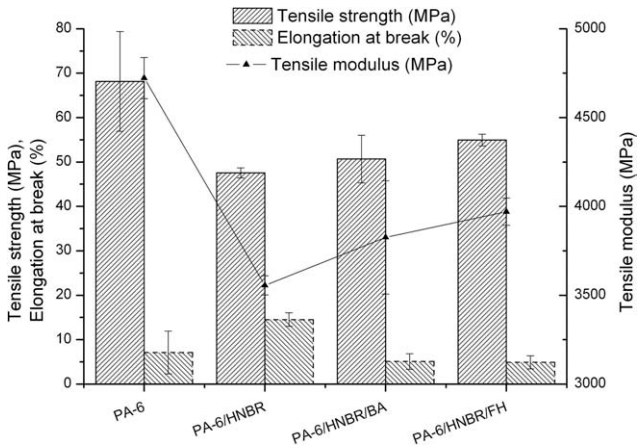

Figure 5 Tensile mechanical characteristics of the systems studied.

RESULTS AND DISCUSSION

Morphology

SEM pictures taken of the PA-6/HNBR blend, PA-6/HNBR/FH, and PA-6/HNBR/BA composite systems are shown in Figures 1–3, respectively. Figure 1 demonstrates that the HNBR particles are dispersed on microscale and rather coarsely in the PA-6 matrix. The FH nanoparticles in a PA-6/HNBR/FH composite are likely located in the PA-6 matrix [cf. Fig. 2(a)], whereas the BA particles are mostly embedded in the HNBR domains (cf. Fig. 3). The TEM picture in Figure 2b confirms that FH particles are mostly dispersed in the matrix and in the PA-6/HNBR interphase. However, some FH stacks can also be resolved in the rather large HNBR domains. XRD results support that the FH is predominantly intercalated (cf. Fig. 4). The shift in the interlayer distance is, however, moderate as it has been changed from 0.92 nm to 1.01 nm. A

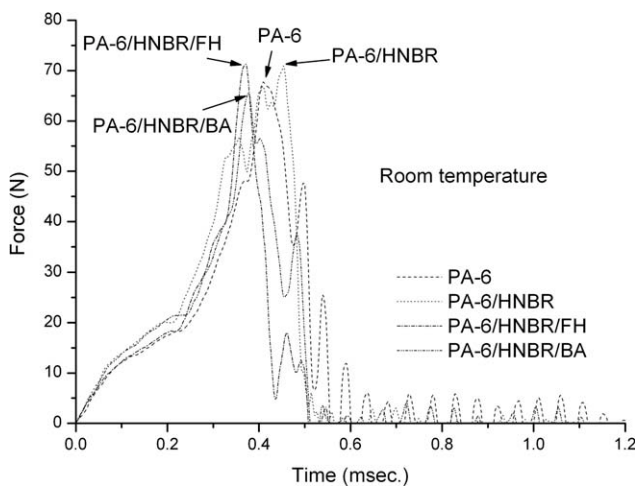

Figure 6 Characteristic force–time curves registered on notched specimens of the systems studied.

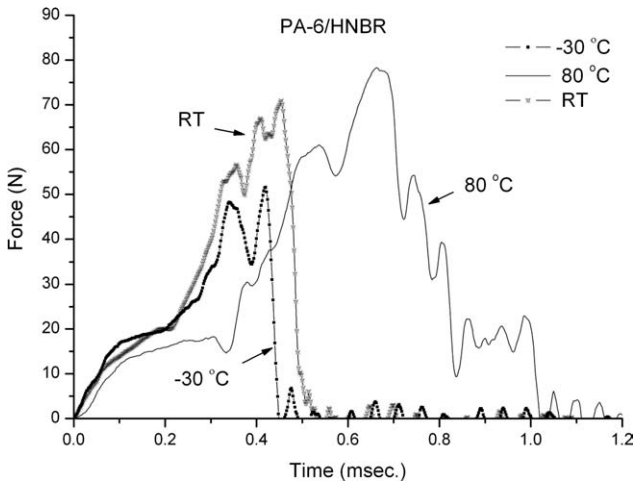

Figure 7 Characteristic force–time curves registered on notched specimens PA-6/HNBR at different testing temperatures.

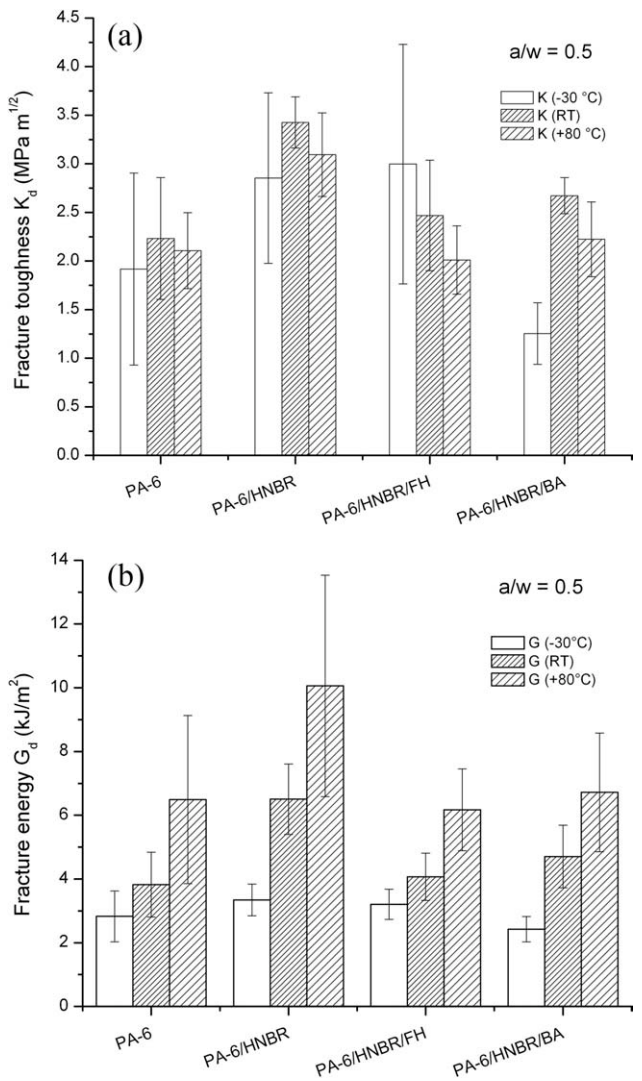

Figure 8 (a) Fracture toughness and (b) energy of the systems studied at different testing temperatures.

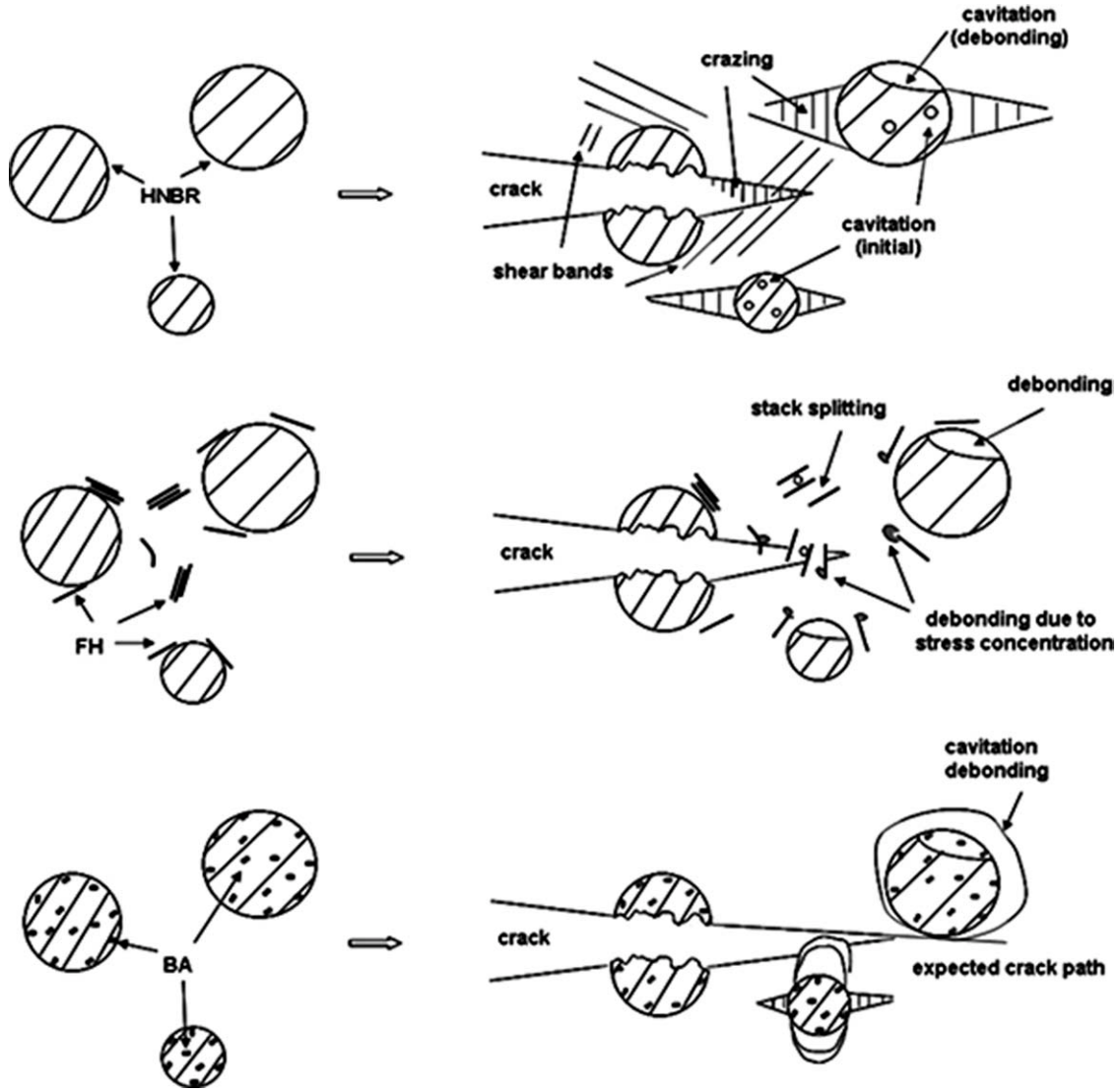

Figure 9 Schemes of the failure modes in PA-6/HNBR, PA-6/HNBR/FH, and PA-6/HNBR/BA, respectively.

similar trend has been reported for polystyrene/FH nanocomposites produced by the water-mediated method.[14]

Tensile response

Tensile mechanical data in form of tensile strength, modulus, and elongation at break are displayed in Figure 5. Due to the rubbery character of the incorporated HNBR, the PA-6/HNBR blend exhibits markedly lower stiffness than the parent PA-6. However, the elongation at break increases prominently by adding HNBR to PA-6. It is usually accepted that rubber domains first cavitate provoking locally a plane strain/plane stress transition in fracture mechanical terms.[8] This supports the development of crazing (with further elongation of the craze fibrils) and superimposed shear yielding, which all enhance the ductility. As expected, the nanoparticle reinforcement leads to increased stiffness and reduced ductility.[6,7] The latter is mainly due to the stress concentration effects of filler agglomerates which cannot be released by matrix-related events (crazing and shear deformation) owing to inhomogeneous filler dispersion. Stress concentration induces filler/matrix debonding and the related voids coalescence causing final, premature fracture.

The nanocomposite containing FH exhibits higher E-modulus than the companion composite containing BA, though the related value remains under that of the neat PA-6. This relative stiffness increment should be traced to the difference in the dispersion characteristics of FH and BA. Recall that FH was intercalated and mostly dispersed in the PA-6 matrix by contrast to BA being located in the HNBR phase (cf. Figs. 2–4). The stiffness data are in agreement with results of dynamic-mechanical thermal analysis as reported in our previous work.[6]

Flexural impact response

Figure 6 displays characteristic fractograms (force as a function of time) for the PA-6, PA-6/HNBR blend and ternary nanocomposites (PA-6/HNBR/FH and PA-6/HNBR/BA). Incorporation of HNBR in PA-6 was accompanied with a shift of the force peak toward higher force and longer time. This already suggests that HNBR worked as toughening agent and enhanced both the Kd and Gd. The presence of nanofillers was associated with a small reduction in both the maximum force peak and fracture time. The effect of testing temperature on the force versus time curves is demonstrated on example of the PA-6/HNBR blend in Figure 7. One can notice that with increasing temperature the time to fracture increases, and parallel to that also the peak force. The largest change in the fracture time occurs between RT and $T = 80°C$ due to the fact that the glass transition temperature of PA-6 has been surpassed at the latter testing temperature. In the first approximation, one can assume that the maximum load in the fractograms increases with increasing testing temperature. Accordingly, one would expect a similar increase in Kd.

The temperature dependence of the fracture toughness and energy is depicted in Figures 8(a,b), respectively. It can be seen in Figure 8(a) that incorporation of HNBR improves the fracture toughness of the PA-6 markedly. Additional presence of nanofillers deteriorated the Kd at all temperatures. The large scatter in the Kd data of PA-6 at $T = -30°C$ was not reduced by HNBR as the glass transition temperature of the latter is slightly above this testing temperature. Kd of the PA-6/HNBR/nanofillers systems was in between of the PA-6 and PA-6/HNBR. The largest difference between the FH- and BA-filled nanocomposites was noticed at $T = -30°C$. This may be linked with the difference in morphology. BA, dispersed in the HNBR, most probably reduces the ability for cavitation of the latter. Note that cavitation of the rubber is the first mechanism of the energy dissipation process in PAs.[8] By contrast, FH stacks in the PA-6 matrix work as fibrous reinforcements and thus increase Kd even at $T = -30°C$.

HNBR incorporation improves Gd, however, prominently only at RT and above—see Figure 8(b). As mentioned before, this is due to the rather high T_g of HNBR (ca. $-25°C$ according to Ref. 15). On the other hand, no enhancement was found in the Gd data of the ternary nanocomposites compared to the parent PA-6 [cf. Fig. 8(b)].

The failure mechanisms, supposed to be at work both under static and dynamic loadings, are summarized in Figure 9 schematically. Note that the matrix-related deformations (i.e., crazing and shear yielding—acting as major energy absorption mechanism in PA-6/HNBR) are suppressed by the presence of both nanofillers. The FH layers and stacks, reinforcing the matrix in PA-6/HNBR/FH system, induce void formation via debonding events. Instead of internal cavitations interfacial debonding occurs in the BA-filled HNBR particles in the PA-6/HNBR/BA system. Both of them trigger a localized crack growth via void coalescence accompanied with reduced ductility.

CONCLUSIONS

This work was devoted to study the structural dependence of the static tensile and dynamic impact properties of toughened and nanoreinforced PA-6. As toughening agent HNBR, whereas as nanofillers FH and BA were used. The nanofillers were dispersed in the HNBR latex which was dried prior to melt compounded with PA-6. Based on the results the following conclusions can be drawn:

Morphology: HNBR was coarsely and microscale dispersed in PA-6. FH, slightly intercalated, was present in PA-6 and in the PA-6/HNBR interphase, whereas BA was mostly located in the HNBR droplets.

Static tensile: Adding of HNBR decreased the stiffness and strength and enhanced the ductility. Additional incorporation of FH and BA nanofillers caused an opposite trend.

Dynamic impact: HNBR improved the fracture toughness and energy, especially above its T_g, of the related blend. The dynamic fracture mechanical properties of the ternary nanocomposites did not differ much from those of the neat PA-6.

References

1. Wilkinson, A. N.; Man, Z.; Stanford, J. L.; Matikainen, P.; Clemens, M. L.; Lees, G. C.; Liauw, C. M. Macromol Mater Eng 2006, 291, 917.
2. Chow, W. S.; Mohd Ishak, Z. A.; Karger-Kocsis, J. Macromol Mater Eng 2005, 290, 122.
3. Kakimoto, M. A.; Takahashi, A.; Tsurumi, T. A.; Hao, J.; Li, L.; Kikuchi, R.; Miwa, T.; Oono, T.; Yamada, S. Macromol Mater Eng 2006, 132, 74.
4. Schartel, B.; Pötschke, P.; Knoll, U.; Abdel-Goad, M. Eur Polym Mater 2005, 41, 1061.
5. Chow, W. S.; Mohd Ishak, Z. A. Exp Polym Lett 2007, 2, 77.
6. Siengchin, S.; Karger-Kocsis, J. Comp Sci Tech 2009, 69, 677.
7. Karger-Kocsis, J. In On the Toughness of "Nanomodified" Polymers and Their Traditional Polymer Composites in "Nano- and Micromechanics of Polymer Blends and Composites"; Karger-Kocsis, J.; Fakirov, S.; Eds.; Hanser: Munich, 2009; Chapter 12, p 425.
8. Paul, D. R.; Bucknall, C. B., Eds. Polymer Blends: Formulation and Performance; John Wiley & Sons: New York, 2000; Vol. 2.
9. Wahit, M. U.; Hassan, A.; Mohd Ishak, Z. A.; Czigány, T. Exp Polym Lett 2009, 3, 309.
10. Bárány, T.; Czigány, T.; Karger-Kocsis, J. Prog Polym Sci 2010, 35, 1257.
11. Ramezani-Dakhel, H.; Garmabi, H. J Appl Polym Sci 2010, 118, 969.
12. Das, P. K.; Ambatkar, S. U.; Sarma, K. S. S.; Sabharwal, S.; Banerji, M. S. Polym Int 2006, 55, 118.
13. Das, P. K.; Ambatkar, S. U.; Sarma, K. S. S.; Sabharwal, S.; Banerji, M. S. Polym Int 2006, 55, 688.
14. Siengchin, S.; Karger-Kocsis, J.; Apostolov, A. A.; Thomann R. J Appl Polym Sci 2007, 106, 248.
15. Xu, D.; Karger-Kocsis, J.; Schlarb, A. K. Exp Polym Lett 2009, 3, 126.